

# Galaxies in SDSS and DEEP2: a quiet life on the blue sequence?

Michael R. Blanton<sup>1</sup>

## ABSTRACT

In the six billion years between redshifts  $z = 1$  and  $z = 0.1$ , galaxies change due to the aging of their stellar populations, the formation of new stars, and mergers with other galaxies. Here I explore the relative importance of these various effects, finding that while mergers are likely to be important for the red galaxy sequence they are unlikely to affect more than 10% of the blue galaxy sequence. I compare the galaxy population at redshift  $z \sim 0.1$  from the Sloan Digital Sky Survey (SDSS) to the sample at  $z \sim 1$  from the Deep Extragalactic Evolutionary Probe 2 (DEEP2). Galaxies are bluer at  $z \sim 1$ : the blue sequence by about 0.3 mag and the red sequence by about 0.1 mag, in  $^{0.1}(u - g)$ . I evaluate the change in color and in the luminosity functions of the two sequences using some simplistic stellar population synthesis models. These models indicate that the luminous end of the red sequence fades less than passive evolution allows by about 0.2 mag. Due to a lack of luminous blue progenitors, “dry” mergers between red galaxies then must create the luminous red population at  $z \sim 0.1$  if stellar population models are correct. The blue sequence colors and luminosity function are consistent with a reduction in the star-formation rate since  $z \sim 1$  by a factor of about three, with no change in the number density to within 10%. These results restrict the number of blue galaxies that can fall onto the red sequence by any process, and in particular suggest that if mergers are catastrophic events they must be rare for blue galaxies.

*Subject headings:* galaxies: evolution

## 1. Motivation

How galaxies form is naturally an important and interesting topic for astronomers, living as we do in the disk of a relatively large and typical galaxy. A well-developed theory of galaxy formation exists, in which galaxies form at the centers of the potential wells of the dark matter halos that are a natural prediction of the current standard Cold Dark Matter (CDM) cosmology. Gasdynamic simulations (e.g. Kereš et al. 2005; Springel et al. 2005; Nagamine et al. 2005) and simpler “semi-analytic” models (e.g. Benson et al. 2003; Nagashima et al. 2005) attempt to make predictions of this theory. The class of predictions I address here involve the change of galaxies (and consequently of the galaxy population) over time. Of course, given the finite age of the Universe, galaxies must change over time, but the predictions are more specific than that and qualitatively point mostly in the same direction: that star formation was higher in galaxies in the past and that their luminosities were larger (Springel & Hernquist 2003; Nagamine et al. 2001).

High redshift galaxy surveys of the past ten or twenty years or so have revealed such changes — indeed, the observations predate the theoretical predictions. The first such observations were in clusters, and indicated that the fraction of blue galaxies has declined markedly in the last 3–4 Gyrs (Butcher &

---

<sup>1</sup> Center for Cosmology and Particle Physics, Department of Physics, New York University, 4 Washington Place, New York, NY 10003

Oemler 1984). Observations of galaxies in the field have indicated that this process occurs in the field as well (Lilly et al. 1995; Cowie et al. 1996; Cohen 2002; Im et al. 2002; Gabasch et al. 2004; Bell et al. 2004; Faber et al. 2005; Willmer et al. 2005). Taken as a whole, these observations have indicated that between redshifts  $z = 1$  and  $z = 0$  galaxies became dimmer and less star-forming.

Here, I present a detailed comparison of the change in the luminosity and color distribution of galaxies between redshifts around  $z \sim 1$  and  $z \sim 0.1$ . At redshift  $z \sim 0.1$  I use the Sloan Digital Sky Survey (SDSS; York et al. 2000) to measure the color and absolute magnitude distribution of galaxies. As Blanton et al. (2003b) demonstrated, the structure of this distribution consists of the well-known red sequence of galaxies (Baum 1959; Faber 1973; Visvanathan & Sandage 1977; Terlevich et al. 2001) and a similar but much broader blue sequence of galaxies. In this paper, I compare this distribution to the corresponding distribution in the Deep Evolutionary Extragalactic Probe 2 (DEEP2; Davis et al. 2003; Faber et al. 2003).

In Section 2, I describe the two data sets. In Section 3 I describe the procedure for the conversion of the SDSS sample into the DEEP2 sample. In Section 4 I compare the SDSS and DEEP2 samples. In Section 5 I present a simple model of the results. In Section 6, I discuss the implications of the models and the data. In Section 7, I present conclusions.

Where necessary, I have assumed cosmological parameters  $\Omega_0 = 0.3$ ,  $\Omega_\Lambda = 0.7$ , and  $H_0 = 100 h$  km s<sup>-1</sup> Mpc<sup>-1</sup> (with  $h = 1$ ). All magnitudes are (unless otherwise noted) AB-relative. Throughout, I will refer to a piece of software, `kcorrect`<sup>1</sup>, for converting between various bandpass systems (Blanton et al. in preparation). Except where noted, I will always be referring to the version of the software labeled `v4_1_4`. Finally, note that most of my comparisons will be in the <sup>0.1</sup>*g* band, which is the SDSS *g* band blueshifted by a factor 1.1, and has virtues extolled below.

## 2. Data

### 2.1. SDSS

The SDSS is taking *ugriz* CCD imaging of 10<sup>4</sup> deg<sup>2</sup> of the Northern Galactic sky, and, from that imaging, selecting 10<sup>6</sup> targets for spectroscopy, most of them galaxies with  $r < 17.77$  mag (e.g., Gunn et al. 1998; York et al. 2000; Abazajian et al. 2003). Automated software performs all of the data processing: astrometry (Pier et al. 2003); source identification, deblending and photometry (Lupton et al. 2001); photometricity determination (Hogg et al. 2001); calibration (Fukugita et al. 1996; Smith et al. 2002); spectroscopic target selection (Eisenstein et al. 2001; Strauss et al. 2002; Richards et al. 2002); spectroscopic fiber placement (Blanton et al. 2003a); and spectroscopic data reduction. Descriptions of these pipelines also exist in Stoughton et al. (2002). An automated pipeline called `idlspec2d` measures the redshifts and classifies the reduced spectra (Schlegel et al., in preparation).

The spectroscopy has small incompletenesses coming primarily from (1) galaxies missed because of mechanical spectrograph constraints (6 percent; Blanton et al. 2003a), which leads to a slight under-representation of high-density regions, and (2) spectra in which the redshift is either incorrect or impossible to determine (< 1 percent). In this context, I note that the mechanical constraints are due to the fact that fibers cannot be placed more closely than 55"; when two or more galaxies have a separation smaller than this distance, one member is chosen independent of its magnitude or surface brightness. Thus, this incomplete-

---

<sup>1</sup><http://cosmo.nyu.edu/blanton/kcorrect>

ness does not bias the sample with respect to luminosity. In addition, there are some galaxies ( $\sim 1$  percent) blotted out by bright Galactic stars, but this incompleteness should be uncorrelated with galaxy properties.

## 2.2. NYU-VAGC

For the purposes of computing large-scale structure and galaxy property statistics, we have assembled a subsample of SDSS galaxies known as the NYU Value Added Galaxy Catalog (NYU-VAGC; Blanton et al. 2005). Here I use the version of that catalog corresponding to the SDSS Data Release 4 (DR4; Adelman-McCarthy et al. 2006). The reader can obtain this catalog at our web site<sup>2</sup>. The main advantage of this catalog is that it accurately and almost completely describes the window function of the SDSS, including the flux limit and completeness as a function of position. Doing so allows statistical studies of galaxies. In this case, I can estimate the maximum volume in which SDSS could have observed each galaxy  $V_{\max}$ , accounting for the flux limits and completeness of the survey.

The sample I use here consists of galaxies with Galactic extinction corrected (Schlegel et al. 1998), Petrosian magnitudes  $14.5 < m_r < 17.6$ , and redshifts  $0.05 < z < 0.15$ . For calculating  $V_{\max}$ , the evolution correction applied is:

$$E(z) = Q_0(1 + Q_1(z - z_0))(z - z_0) \quad (1)$$

with  $z_0 = 0.1$ ,  $Q_0 = 2.8$  and  $Q_1 = -1.8$ . For the selection and  $V_{\max}$  determination I use  $K$ -corrections from `kcorrect v3.4` (Blanton et al. 2003); note that this is an earlier version than I use for the rest of the calculations in this paper, but for these purposes the differences are tiny (percent-level). In other respects I select this sample according to the Main sample criteria that Strauss et al. (2002) describe.

When necessary below, we will  $K$ -correct the magnitudes to  $^{0.1}u$  and  $^{0.1}g$  bands, the SDSS  $u$  and  $g$  bands shifted to match their rest frame coverage at  $z = 0.1$ , the typical redshift in our sample. This choice is wise because these bandpasses also are close in wavelength to the DEEP2 bandpasses in the rest frame. For example, the effective wavelength of  $^{0.1}u$  and  $^{0.1}g$  are 3223 Å and 4245 Å respectively, while for  $R$  and  $I$  the effective rest frame wavelengths at redshift  $z = 1$  are 3297 Å and 4059 Å respectively. Note that  $^{0.1}g$  is also fortuitously close to the rest frame  $B$  band (4344 Å) of Bessell (1990).

In order to compare our results here to other related results, one can use the approximate relationships:

$$\begin{aligned} ^{0.1}u &= u + 0.33 + 0.32[(u - g) - 1.26] \\ ^{0.1}g &= g + 0.32 + 0.25[(u - g) - 1.26] \\ ^{0.1}g &= B + 0.07 + 0.06[(B - V) - 0.59] \end{aligned} \quad (2)$$

In particular, note the small color term between  $^{0.1}g$  and  $B$ . (All of these magnitudes are AB relative).

## 2.3. DEEP2

As the redshift  $z \sim 1$  sample, I use DEEP2 (Davis et al. 2003; Faber et al. 2003). The DEEP2 team took Canada-France-Hawaii Telescope images in  $B$ ,  $R$ , and  $I$ . Coil et al. (2004) describe the construction of a catalog based on these data. DEEP2 used a set of color criteria (discussed more fully below) to select

---

<sup>2</sup><http://sdss.physics.nyu.edu/vagc>

galaxies likely to have redshifts  $z > 0.7$ . Using the DEIMOS spectrograph on Keck 2, they obtained spectra for  $> 10,000$  of these galaxies.

DEEP2 has released an initial set of data (DR1).<sup>3</sup> These data include the observations in their 2002 observing season and have 5,191 high quality redshifts (quality  $\geq 3$ ), 2,976 of them in the redshift range  $0.8 < z < 1.2$ .

To obtain rest-frame quantities from this data, I use the routine `deep_kcorrect` from `kcorrect` to convert to SDSS  $^{0.1}u$  and  $^{0.1}g$  bands, which are close in the rest frame to the  $R$  and  $I$  DEEP2 observations. The routine `deep_kcorrect` fits a simple spectral model to the  $B$ ,  $R$ , and  $I$  observations, and calculates for the model the ratio between the rest-frame  $^{0.1}u$  or  $^{0.1}g$  band flux and the observed frame  $R$  or  $I$  band flux. Then it multiplies that ratio to the observed  $R$  or  $I$  flux to obtain the estimated rest frame  $^{0.1}u$  or  $^{0.1}g$  flux. When I use similar code to convert the observed  $R$  band flux to the rest-frame  $B$  band flux, I obtain results very similar to those in Figure A15 of Willmer et al. (2005), demonstrating that I am using  $K$ -corrections similar to those used by the DEEP2 team.

#### 2.4. DEEP2 $V_{\max}$ values

For each DEEP2 galaxy in the redshift range  $0.8 < z < 1.2$ , I also calculate a maximum volume over which it could be detected:

$$V_{\max} = \frac{1}{3} \int d\Omega \int_{0.8}^{1.2} dz \frac{d[D_c(z)^3]}{dz} g(z, z_{\text{act}}, B, R, I) \quad (3)$$

where the angular integral is over the full DR1 area,  $z_{\text{act}}$  is the actual redshift in question, and the function  $g(z, z_{\text{act}}, B, R, I)$  expresses the probability of selecting a galaxy at the given redshift  $z$  given its SED (which I estimate from  $z_{\text{act}}$  and its  $B$ ,  $R$ , and  $I$  magnitudes).

To calculate the integral over angle, I would have liked to have simply taken geometrical descriptions of the masks and calculated the area, but the DR1 release did not include descriptions I could interpret. So I instead took a simpler and approximate approach. I counted objects from the full photometric DEEP2 catalog within  $45''$  of any object in an observed DR1 mask, finding a total  $N_m$  matched objects. I then counted the objects in the full DEEP2 photometric catalog, finding a total  $N_p$  over an area  $\Omega_p$ . The DEEP2 spectroscopic area is then approximately  $\Omega = N_m \Omega_p / N_p = 1.94 \times 10^{-4}$  square radians, or 0.63 sq deg (unweighted by completeness).

To calculate the integral over redshift, I use a Monte Carlo approach. For each object, I randomly choose 12,000 values of redshift  $z$  between 0.8 and 1.2, distributed according to volume. For each redshift, I calculate what the magnitudes of the object would be using the `deep_kcorrect` routine of `kcorrect`. I then apply the magnitude and color cuts of DEEP2:

$$\begin{aligned} B - R &< 2.35(R - I) - 0.25 \quad , \text{ or} \\ R - I &> 1.15 \quad , \text{ or} \\ B - R &< 0.50. \end{aligned} \quad (4)$$

in addition to  $R < 24.1$ .

---

<sup>3</sup><http://deep.berkeley.edu/DR1>

Furthermore, I apply the estimated incompleteness of DEEP2. Willmer et al. (2005) estimate the magnitude of incompleteness due to surface brightness effects (5–7%), star-galaxy separation errors ( $\sim 10\%$ ), and the unobserved  $B$ -band dropouts (4–8%). I ignore these effects here. However, I need to account for two important effects that Willmer et al. (2005) do discuss. First, because of an early change in the selection criteria, the number of targets selected to be targeted is a function of  $I$  magnitude (J. Newman, private communication). Second, redshift success is a function of color. Thus, I evaluate as a function of  $R$  and  $R - I$  the fraction of possible galaxies that were observed ( $f_t(R, R - I)$ ) and the fraction of observed galaxies with successful redshifts ( $f_g(R, R - I)$ ). I obtain results similar to those in Figure 5 of Willmer et al. 2005. In fact, according to Willmer et al. (2005), most of the blue galaxies without successful redshifts in the DEEP2 survey are at  $z > 1.4$ , so I will simply set  $f_g(R, R - I) = 1$  for  $R - I < 0.9$ . I select random redshifts from the set of 12,000 with probabilities depending on the predicted observed colors equal to the product  $f_t(R, R - I)f_g(R, R - I)$ .

Then the estimate for  $V_{\max}$  for each galaxy is the volume between redshifts  $z = 0.8$  and  $z = 1.2$ , times the fraction of the 12,000 selected redshifts which pass the above selection.

### 3. SDSS as it would appear in DEEP2

The SDSS catalog contains measurements in the  $u$ ,  $g$ ,  $r$ ,  $i$ , and  $z$  bands for galaxies at redshifts  $z \sim 0.1$ . Meanwhile, DEEP2 contains measurements in  $B$ ,  $R$ , and  $I$  for galaxies at redshifts  $z \sim 1$ . Furthermore, the SDSS has a simple flux limit in the  $r$ -band (there is a surface brightness selection as well, but as Blanton et al. 2005 show it is unimportant for the range of luminosities I consider here). Meanwhile, DEEP2 is selected in the  $R$  band, which is comparable in rest-frame wavelength to the  $u$  band for the SDSS galaxies. Any comparison between the two surveys must account for these differences. I do so here as follows.

First, one must correct the SDSS sample for the flux selection, in order to be dealing with an effectively volume-limited sample. I do so by assigning a probability of selection to each galaxy that is proportional to  $1/V_{\max}$ . Then I randomly select a large set of galaxies (with replacement) from the original sample.

Second, I assign each galaxy a redshift in the range  $0.5 < z < 1.5$ , distributed uniformly in comoving volume. Given its redshift I determine for each selected galaxy what its  $B$ ,  $R$ ,  $I$  magnitudes would be using the routine `sdss2deep` contained in `kcorrect` (Blanton et al. in preparation). I use the SDSS “model” fluxes and uncertainties to fit a spectral energy distribution (SED) to each galaxy. It calculates the flux ratio between each DEEP2 band and the nearest SDSS band in wavelength (the SDSS bands for the rest-frame at the actual redshift of the galaxy and the DEEP2 band for the rest-frame at the assigned redshift). It then multiplies that ratio to the flux in the nearest SDSS band to obtain an estimate of the DEEP2 flux. The DEEP2 and SDSS filter curves I assume are given in the `kcorrect` product.

I have tested this method by taking the converted galaxies, applying to them the DEEP2  $K$ -corrections I describe above, and comparing the resulting  $^{0.1}u$  and  $^{0.1}g$  absolute magnitudes to what one would find by  $K$ -correcting directly from the SDSS data. In the mean, these two methods agree to about 0.03 mag, with about 0.05 scatter. This test also provides a consistency check on our  $K$ -corrections of the DEEP2 galaxies.

Third, I apply the color, magnitude, and incompleteness selection to the sample, as described in Section 2.4.

Figure 1 shows the  $B - R$  and  $R - I$  distributions for the resulting sample. One can see that, indeed, the distribution cuts off sharply below redshift  $z = 0.7$ , just as the DEEP2 team intended. In addition, the

red sequence of galaxies declines at the highest redshifts, purely due to the selection effects.

It is worth noting that the  $B$  band at redshift  $z = 1$  is close to the near ultra-violet (NUV) band of the Galaxy Evolution Explorer (GALEX), much bluer than there are observations for most of the SDSS galaxies. However, Blanton et al. (in preparation) show that the fits to the SDSS bands correctly predict the GALEX NUV bands to within 0.5 mag scatter and 0.2 mag in the mean. So the clear separation into two populations in  $B - R$  is real.

## 4. Change in the galaxy population

### 4.1. Colors as a function of redshift

Figure 2 shows the same quantities as Figure 1, but for the actual DEEP2 galaxies. Clearly there is a huge difference in the two populations. The DEEP2 sample has a much weaker red sequence relative to the local population. In addition, its blue sequence is bluer.

### 4.2. Comparison of the color-magnitude diagram

To quantify these differences, I take DEEP2 galaxies in the redshift range  $0.8 < z < 1.2$  and correct them to the rest frame  $^{0.1}u$  and  $^{0.1}g$  bands. For uniformity, I do exactly the same thing to galaxies in the SDSS prediction (rather than use the SDSS estimates of the magnitudes directly). Again, for this task I use a routine (`deep_kcorrect`) from `kcorrect`.

Figure 3 shows the result: the top panel shows the prediction from SDSS in the case that there is no change in the galaxy population; the bottom panel shows the actual DEEP2 observations. The upper solid line in each plot is the locus of the red sequence in the SDSS. The lower solid line is the locus of the blue sequence in the SDSS. The dashed lines are the corresponding fits to the DEEP2 sample. Table 1 gives the parameters of the fits to the data.

The red sequence does not shift *very* much between SDSS and DEEP2 — it is about 0.1 mag bluer at high redshift. On the other hand the blue sequence shifts considerably. For example, the dashed line is the locus of the blue sequence in DEEP2, which is 0.3 mag bluer in  $^{0.1}(u - g)$  than the SDSS locus.

For luminous galaxies ( $M_{0.1g} - 5 \log_{10} h < -20$ ), for which the selection effects are less important, Figure 4 shows the distribution of color in both the actual (solid histogram) and the SDSS-predicted (dotted histogram) samples. Here one clearly sees the shift in the red and blue sequences, as well as the overwhelming dominance of the blue sequence at high redshift. The fraction of red galaxies at redshift  $z = 1$  is about 0.24, whereas the corresponding fraction in the redshift  $z = 0.1$  sample is 0.47. This change is the effect Butcher & Oemler (1984) discovered, but in the field.

In what follows, I will show that it is reasonable for both the red and blue sequences to passively evolve. If we approximately account for that evolution by using a cut  $M_{0.1g} - 5 \log_{10} h < -20$  in the SDSS sample, we find the red fraction is about 0.33, indicating that much of the shift in the color distribution is due to observing (at fixed absolute magnitude) lower stellar mass objects at higher redshift.

### 4.3. Comparison of luminosity functions

While Figures 3 and 4 show the raw distributions of DEEP2 galaxies, I can also attempt to correct the galaxies for the flux and color limits by weighting each galaxy by  $1/V_{\max}$  as calculated in Sections 2.2 and 2.4. Weighting by this value allows each galaxy to contribute its number density, and the sum of  $1/V_{\max}$  for some set of galaxies should thus be the number density of galaxies in that set. I divide the galaxies into red and blue galaxies for three different samples:

1. the original SDSS sample;
2. the converted SDSS sample, as described in Section 3; and
3. the DEEP2 sample.

I then calculate the luminosity functions of each sample: the number density per unit magnitude and volume as a function of absolute magnitude.

Figure 5 shows the results of this calculation, with the red galaxy luminosity function in the top panel and the blue galaxy luminosity function in the bottom panel. Table 2 lists the original SDSS luminosity function and the DEEP2 luminosity function in these figures. The original SDSS sample (dotted histogram) and the converted SDSS sample (thin solid histogram) agree for  $M_{0.1g} - 5 \log_{10} h < -19$ . This agreement demonstrates that in that regime one can correct the DEEP2 survey for its explicit color cuts (whether I have correctly described the incompletenesses that I have also corrected for cannot be addressed by this comparison). As a further check, Figure 6 compares these results to those of Willmer et al. (2005) (and also in Faber et al. 2005, and good agreement is found. Similarly good agreement is found between both these results and the COMBO-17 results of Bell et al. (2004), as Faber et al. (2005) show.

One can explore the differences between these luminosity functions in two ways. First, one can simply ask how much one needs to shift the absolute magnitudes and the overall number density at  $z \sim 1$  to match the luminosity functions at  $z \sim 0.1$ , keeping the shape of the luminosity function fixed. I determine the optimal shift  $\Delta M_{0.1g} = M_{0.1g, \text{SDSS}} - M_{0.1g, \text{DEEP2}}$  and offset  $f_{\text{off}} = \rho_{\text{SDSS}}/\rho_{\text{DEEP2}}$  by minimizing  $\chi^2$  and estimate the uncertainties with a jackknife technique. Table 3 lists the best-fit shifts and uncertainties. Figure 7 shows the resulting luminosity function at redshift  $z \sim 0.1$ . The blue sequence is consistent with a simple fading by about  $1.0 \pm 0.1$  mag, with a factor of  $1.2 \pm 0.14$  offset in the overall number density. On the other hand, it is difficult to avoid a change in the overall number density of red galaxies, as previous workers have found. The best fit is about a factor of two.

Second, one can require that the numbers of galaxies be roughly conserved by fitting for a single shift in magnitude of all galaxies, but allowing some galaxies to transfer from the red sequence to the blue sequence by some process. The best fit for a shift is  $\Delta M_{0.1g} = 0.6 \pm 0.05$ , with a fraction of blue galaxies transferring to the red sequence of  $0.25 \pm 0.05$ . Figure 8 shows the result. This picture is somewhat simpler than the first, not requiring the majority of red galaxies at low redshift to have formed from many mergers objects below the detection limit. Note that the number densities of the most luminous red galaxies are hardly affected by the transfer from the blue sequence, and that the number densities of these objects are in agreement if the luminosity evolution is only 0.6 mag (which is hard to get from standard passive evolution scenarios).

## 5. A simple model of the color-magnitude diagram and the luminosity functions

In the previous section, I found that between redshift  $z = 1$  and  $z = 0$  the galaxies on both the blue sequence and red sequence become redder and less luminous. Here I try to interpret these results in some simple ways. My approach is *not* to hypothesize about the fundamental physical processes at work — which might include accretion, ram pressure stripping, and merging, among others — but to simply ask what these observations may tell us about the star-formation histories.

### 5.1. Description of the model

As a tool, I define a simple set of models for the star-formation history of galaxies. All of the predictions are based on spectra produced for these models in the stellar population synthesis package of Bruzual & Charlot (2003) using the Chabrier (2003) stellar initial mass function (IMF).

The model for the blue sequence consists of an initial burst of duration 1 Gyr starting at the beginning of the Universe, followed by quiescent star-formation until  $z = 1$  (5.8 Gyrs). I use four such models, with initial burst star-formation rates 2, 15, 50, and 120 times the quiescent rate (to land on the blue sequence at  $z \sim 1$ ), and with metallicities 30%, 50%, 70% and 90% solar (to land on the red sequence at  $z \sim 0.1$  if star-formation ends). I set the normalizations set such that the model galaxies follow the blue sequence at  $z = 1$ . After  $z = 1$  I allow three alternatives: a cutoff in the star-formation, a reduction in the quiescent star-formation rate by a factor of three, and a continuation of the quiescent star-formation at a constant rate.

The left-hand panels Figure 9 shows the evolution in absolute magnitude (top panel) and color (bottom panel) for blue sequence models with burst star-formation rates of 2 (thin line) and 120 (thick line) times the quiescent rate. Each of the three alternatives are shown for the behavior after redshift  $z = 1$ . In each case, a reduction in star-formation increases the rate of fading and reddening. A complete cutoff in star-formation puts a galaxy onto the red sequence very rapidly, in around 1 Gyr, and leads to the most rapid fading. A continuation of star-formation at a constant rate leads to nearly constant colors and absolute magnitudes. Meanwhile, a simple reduction in the star-formation rate leads to a rapid reddening of the color (but not all the way onto the red sequence) and a reduction in the luminosity. For the small initial burst, the change in absolute magnitude after a reduction of the star-formation rate is about 0.90 mag, and for the large initial burst it is about 0.85 mag. The changes in  $^{0.1}(u - g)$  color are 0.15 mag and 0.2 mag respectively. Taken together and accounting for the slope of the color magnitude diagram in Table 1, this makes the shift in color at fixed absolute magnitude about 0.3, approximately that observed.

The rapidity of the reaction to any change in star-formation rates indicates that bimodality in the color distribution is a generic feature arising from stellar population synthesis. As long some galaxies can have star-formation rapidly cut off, it is difficult to avoid a strong separation in color-space from those who have had such a cut off and those who have not.

The right-hand panel shows my model for a typical red sequence galaxy, a stellar population of solar metallicity born in a 1 Gyr burst at the beginning of the Universe, passively evolving thereafter. We will see from the examination of the blue sequence models that blue sequence galaxies whose star-formation ends abruptly can rapidly move onto the red sequence, so by no means am I suggesting that this red sequence model describes the star-formation of all red sequence galaxies. However, as long as they sit on the red sequence, it does not matter much how they got there: their evolution in color and magnitude is about the

same. Between redshifts  $z = 1$  and  $z = 0$  the absolute magnitude shifts by 0.80 mag and the color by about 0.15. Because the burst in this model is as early as possible, it represents about the minimum evolution one could expect from these models.

## 5.2. Comparison to the color-magnitude diagram

Figure 10 shows the results of these star-formation histories at various points during the Universe. The bottom panel shows all the models at redshift  $z = 1$ . By design, the normalizations, initial bursts strengths, and metallicities of the blue sequence models are set so all of the models actually do sit on the blue sequence.

The top panel of Figure 10 shows all the models at redshift  $z = 0$ . For the blue sequence models, the figure shows the results of the different hypotheses. Obviously, the case in which the star-formation is abruptly cut off results in all of the models sitting near the red sequence. The case in which star-formation continues at a constant rate results in bluer colors than is typical. The case in which star-formation declines by a factor of three results in models sitting on the blue sequence at redshift  $z = 0.1$ . Obviously, I chose a factor of three to guarantee this, and the exact level of decline depends on the metallicities and dust contents, but it is fairly clear that the star-formation rates of typical blue sequence galaxies has declined with time.

By design, I have chosen the metallicity of the red sequence model to land near the red sequence at both redshift  $z = 1$  and  $z = 0$ . I note in passing, but do not dwell on, the fact that to achieve the redder colors at the tip of the red sequence, I must assume higher metallicities, which will evolve more quickly in color at low redshift than observed. I choose not to dwell on this difficulty because the detailed evolution of the colors of red galaxies almost surely depend on their abundance of alpha-elements, in a way that nobody can yet reliably predict.

## 5.3. Comparison to the luminosity function

What do these models say about the luminosity functions? From the models, and based on the change in color, I expect the blue sequence to fade by about 0.9 mag, and this fading is extremely close to what is observed (if the number density is roughly fixed). For example, the fit in Figure 7 shows the result of fading the blue sequence luminosity function by around this much, with about a 20% increase in the number density. There is therefore probably no large fraction of galaxies lost from the blue sequence due to catastrophic events such as mergers or ram pressure stripping. For example, if I impose a fixed shift of 0.9 mag on the blue sequence, and fit for the scale change in the number density ( $f_{\text{off}}$ ) I find  $1.1 \pm 0.1$ , as listed in Table 3.

On the red sequence, the passive fading of almost any population, regardless of metallicity or previous star-formation history, is about 0.80 mag. Table 3 shows that such fading produces a red luminosity function with about 50% the normalization of the low redshift red galaxy luminosity function. As Bell et al. (2004) conclude, if one thinks that red galaxies fade passively, their number densities must be boosted considerably over time by some process.

In general, these models predict more passive evolution than the red sequence luminosity function evolution can tolerate. In addition, because these models invoke a very old burst, they represent a minimum passive evolution rate (given the IMF choice). Thus, if one trusts these models and the relative absolute photometry at the 0.2 mag level, these results require growth along the red sequence due to mergers, low

level star-formation, or migration from the blue sequence.

#### 5.4. Caveats to the comparisons

Of course, the model here is extremely simplistic but it would not pay to create a more baroque model given the data set I use here. For example, the metallicity of galaxies is definitely a function of absolute magnitude, but this change has little effect on the prediction of the  $^{0.1}(u - g)$  colors of the star-forming galaxies on the blue sequence. Another way of stating this fact is that if I imposed a mass-metallicity relationship in the models, I would simply have chosen different burst strengths to put the model galaxies on the blue sequence at redshift  $z = 1$ . The metallicity does affect where the galaxies end up on the red sequence, but having only the  $^{0.1}(u - g)$  color gives us no handle on what these metallicities really are anyway.

In addition, the change in location of the blue sequence may not be a change in star-formation rate, but simply a difference in the amount of dust in the galaxies. For the Milky Way dust law, 1 mag of extinction in the  $^{0.1}g$ -band reddens galaxies by 0.3 mag in  $^{0.1}(u - g)$ . Given that star-forming galaxies today are believed to have internal extinction of order 1 mag, if *all* of the change in color of the sequence is due to an increase in the dust content it implies that galaxies at redshift  $z = 1$  have near zero dust extinction — which is possible but unlikely.

There are observational caveats, as well. For a number of reasons, the DEEP2 and SDSS magnitudes are not necessarily comparable. First, this comparison requires the AB calibration for both surveys to be good to significantly better than 0.05 mag, which I consider here to be likely. Second, the galaxy photometry is also not necessarily consistent between the surveys. Although the colors are likely to be robust, at the 0.05 mag level the overall normalization of galaxy magnitudes can depend on the method of calculation. This problem is probably most acute on the red sequence, where there are a significant number of de Vaucouleurs galaxies (for exponential galaxies most measures of flux contain all of it). The DEEP2 survey used aperture magnitudes with radii that for redshift  $z = 1$  galaxies correspond to about  $3r_{50}$  ( $r_{50}$  is typically  $3-4 h^{-1}$  kpc for reasonably luminous red galaxies, and the angular size of the apertures were about  $1''.5$ ), which is close to the same as the SDSS Petrosian aperture. The difference, empirically, between the SDSS Petrosian fluxes and the SDSS model fluxes (used here) is about 5%, in the sense that the model fluxes are slightly brighter. Therefore, I am reasonably confident that the DEEP2 and SDSS magnitudes are consistent at the required level.

A second observational caveat is that there may be selection effects eliminating low luminosity red galaxies preferentially, since they tend to be low in surface brightness. Since I do account for the spectroscopic incompleteness as a function of color and magnitude, the most likely culprit here would be a dependence of the photometric completeness on surface brightness. Such a dependence could preferentially bias us against the lowest luminosity red galaxies the most. Short of reimaging the area in question or reanalyzing the photometry itself, one does not have much hope of estimating the magnitude of such an effect or determining if it exists.

Finally, a large uncertainty is simple cosmic variance. The high redshift sample only consists of a volume of about a few times  $10^5 h^{-3} \text{ Mpc}^3$  (and smaller than that for the fainter galaxies in this sample). Such a volume only one or two large clusters in it even at low redshift. Thus, I don't expect that the sample will span the range of cosmic structures or even necessarily constitute a fair sample yet.

## 6. Discussion

### 6.1. A quiet life for the blue sequence

The most striking result here is the mild evolution of the blue sequence, which is consistent with a constant number density to within  $\sim 10\%$ , and a simple decline of the star-formation rate by an amount which is consistent with the change in the color of the blue sequence.

The mild evolution of the blue sequence appears inconsistent with both theoretical predictions and observations of merger rates that suggest that  $> 50\%$  of all galaxies undergo a merger between redshifts  $z = 1$  and  $z = 0$  (Baugh et al. 1996; Le Fèvre et al. 2000; Bell et al. 2004, 2005). If such mergers cause galaxies to leave the blue sequence, between redshifts  $z = 1$  and  $z = 0.1$  the blue sequence would decline a factor of two, which my results suggest it does not. To reconcile the results here with such a high merger rate requires replenishing the blue sequence from some other source (such as former *red* sequence galaxies that acquire new gas?).

On the other hand, other direct observational measurements of the merger histories suggest relatively low numbers of recent mergers, closer to  $10\%$  (Patton et al. 2002; Bundy et al. 2004; Lin et al. 2004). I will not attempt here to reconcile various measurements of the numbers of observed mergers in the Universe. Suffice it to say that measuring pair counts and their change over time is fraught with systematic worries, such as projection effects, Malmquist-type biases, and  $K$ -correction related selection effects. Furthermore, estimating merger rates from pair counts involves assumptions about the time scales of the mergers.

My results here are much more indirect than direct counting of pairs, but suggest that if mergers are catastrophic events for blue galaxies, there cannot have been a large number of them, favoring those results which find a low merger rate (for blue galaxies).

### 6.2. Merging probably required on the red sequence

Meanwhile, the red sequence appears to grow considerably in this time period. Two methods of growing the red sequence seem possible: the migration of blue galaxies to the red sequence due to a cut-off in their star-formation and dry mergers between red galaxies.

As Figure 9 shows, a sharp cutoff in star-formation of a blue sequence galaxies allows it to migrate within 1 Gyr to the red sequence. To get enough galaxies to undergo this process and populate the faint end of the red sequence at redshift  $z = 0.1$  one needs  $25\%$  of the blue population to migrate, which is very marginally allowed. However, to get enough galaxies to populate the bright end of the red sequence at redshift  $z = 0.1$  one cannot rely on migration from the blue sequence, since there are not enough luminous blue galaxies at redshift  $z = 1$ . Instead, one of three things must be true: passive evolution is  $0.2$  mag slower than the scenarios I present here, which are about as slow as current models allow; the fluxes of the SDSS and DEEP2 galaxies are inconsistent in an absolute sense by  $0.2$  mag, which is unlikely; or the luminous red galaxies grow by dry mergers.

In the case of the red galaxies, high merger rates in the observations improve the consistency checks. For example, Bell et al. (2005) estimate based on seven observed close pairs between  $0 < z < 0.7$  that every galaxy on the red sequence merges about once, which may be enough to do the job.

## 7. Conclusions

I have presented a comparison of the low redshift ( $z \sim 0.1$ ) SDSS data with the high redshift ( $z \sim 1$ ) DEEP2 data. In general, the data suggest a quiet life for most galaxies on the blue sequence, with fewer than 10% being destroyed between those two epochs. It remains for better quantitative predictions of  $\Lambda$ CDM than currently exist to determine whether that theory is consistent with this relatively peaceful history.

In particular, the data alone indicate that:

1. the red sequence of galaxies is redder by about 0.1 mag in the low redshift data;
2. the blue sequence of galaxies is redder by about 0.3 mag in the low redshift data;
3. the change in the blue sequence luminosity function is consistent with pure fading; and
4. the change in the red sequence luminosity function requires something more complex, perhaps an increase in number density.

I have further interpreted these results in terms of simple models for the star-formation histories of galaxies. From these models I conclude:

1. that galaxies migrate quickly (1 Gyr) to the the red sequence when their star formation is sharply cut off;
2. the colors and luminosities of blue sequence galaxies are consistent with a decline in star-formation rate by about a factor of three in the last 8 Gyrs;
3. that consistency on the blue sequence suggests that to within  $\sim 10\%$  mergers do not reduce the blue sequence of galaxies, contradicting predictions but in less obvious contradiction to direct observations of mergers; and
4. absent errors in the models or photometry at the 0.2 mag level, the data requires mergers to produce the luminous end of the red sequence.

It is worth contrasting the change of the galaxy population with time to the change of the population with environment, since it illuminates a mystery regarding the latter. As Hogg et al. (2004) and others find, the red and blue sequences of galaxies do not change with environment, they are simply differently populated. In contrast, I find here that the red and blue sequences do change with time. Thus, the analogy often invoked that underdense regions are in some sense “younger” regions of the Universe is not a good analogy — we can observe the Universe when it was younger and it looks quite different than do underdense regions today. This result supports the notion that the blue galaxies in dense regions had on average about the same formation epoch and subsequent history as blue galaxies in underdense regions.

Funding for the DEEP2 survey has been provided by NSF grant AST-0071048 and AST-0071198.

(Some of) The data presented herein were obtained at the W.M. Keck Observatory, which is operated as a scientific partnership among the California Institute of Technology, the University of California and the National Aeronautics and Space Administration. The Observatory was made possible by the generous financial support of the W.M. Keck Foundation. The DEEP2 team and Keck Observatory acknowledge

the very significant cultural role and reverence that the summit of Mauna Kea has always had within the indigenous Hawaiian community and appreciate the opportunity to conduct observations from this mountain.

Funding for the creation and distribution of the SDSS Archive has been provided by the Alfred P. Sloan Foundation, the Participating Institutions, the National Aeronautics and Space Administration, the National Science Foundation, the U.S. Department of Energy, the Japanese Monbukagakusho, and the Max Planck Society. The SDSS Web site is <http://www.sdss.org/>.

The SDSS is managed by the Astrophysical Research Consortium (ARC) for the Participating Institutions. The Participating Institutions are The University of Chicago, Fermilab, the Institute for Advanced Study, the Japan Participation Group, The Johns Hopkins University, the Korean Scientist Group, Los Alamos National Laboratory, the Max-Planck-Institute for Astronomy (MPIA), the Max-Planck-Institute for Astrophysics (MPA), New Mexico State University, University of Pittsburgh, University of Portsmouth, Princeton University, the United States Naval Observatory, and the University of Washington.

## REFERENCES

- Abazajian, K. et al. 2003, *AJ*, 126, 2081
- Adelman-McCarthy, J. et al. 2006, *ApJS*, in press (astro-ph/0507711)
- Baugh, C. M., Cole, S., & Frenk, C. S. 1996, *MNRAS*, 283, 1361
- Baum, W. A. 1959, *PASP*, 71, 106
- Bell, E. F., Wolf, C., Meisenheimer, K., Rix, H.-W., Borch, A., Dye, S., Kleinheinrich, M., Wisotzki, L., & McIntosh, D. H. 2004, *ApJ*, 608, 752
- Bell, E. F. et al. 2005, *ArXiv Astrophysics e-prints*
- Benson, A. J., Bower, R. G., Frenk, C. S., Lacey, C. G., Baugh, C. M., & Cole, S. 2003, *ApJ*, 599, 38
- Bessell, M. S. 1990, *PASP*, 102, 1181
- Blanton, M. R., Brinkmann, J., Csabai, I., Doi, M., Eisenstein, D. J., Fukugita, M., Gunn, J. E., Hogg, D. W., & Schlegel, D. J. 2003, *AJ*, 125, 2348
- Blanton, M. R., Lin, H., Lupton, R. H., Maley, F. M., Young, N., Zehavi, I., & Loveday, J. 2003a, *AJ*, 125, 2276
- Blanton, M. R. et al. 2003b, *ApJ*, 594, 186
- Blanton, M. R. et al. 2005, *AJ*, 129, 2562
- Blanton, M. R. et al. 2005, *ApJ*, 631, 208
- Bruzual, A. G. & Charlot, S. 2003, *MNRAS*, 344, 1000
- Bundy, K., Fukugita, M., Ellis, R. S., Kodama, T., & Conselice, C. J. 2004, *ApJ*, 601, L123
- Butcher, H. R. & Oemler, A. 1984, *ApJ*, 285, 426
- Chabrier, G. 2003, *PASP*, 115, 763

- Cohen, J. G. 2002, *ApJ*, 567, 672
- Coil, A. L., Newman, J. A., Kaiser, N., Davis, M., Ma, C.-P., Kocevski, D. D., & Koo, D. C. 2004, *ApJ*, 617, 765
- Cowie, L. L., Songaila, A., Hu, E. M., & Cohen, J. G. 1996, *AJ*, 112, 839
- Davis, M., Faber, S. M., Newman, J., Phillips, A. C., Ellis, R. S., Steidel, C. C., Conselice, C., Coil, A. L., Finkbeiner, D. P., Koo, D. C., Guhathakurta, P., Weiner, B., Schiavon, R., Willmer, C., Kaiser, N., Luppino, G. A., Wirth, G., Connolly, A., Eisenhardt, P., Cooper, M., & Gerke, B. 2003, in *Discoveries and Research Prospects from 6- to 10-Meter-Class Telescopes II*. Edited by Guhathakurta, Puragra. *Proceedings of the SPIE*, Volume 4834, pp. 161-172 (2003)., 161–172
- Eisenstein, D. J. et al. 2001, *AJ*, 122, 2267
- Faber, S. M. 1973, *ApJ*, 179, 731
- Faber, S. M., Phillips, A. C., Kibrick, R. I., Alcott, B., Allen, S. L., Burrous, J., Cantrall, T., Clarke, D., Coil, A. L., Cowley, D. J., Davis, M., Deich, W. T. S., Dietsch, K., Gilmore, D. K., Harper, C. A., Hilyard, D. F., Lewis, J. P., McVeigh, M., Newman, J., Osborne, J., Schiavon, R., Stover, R. J., Tucker, D., Wallace, V., Wei, M., Wirth, G., & Wright, C. A. 2003, in *Instrument Design and Performance for Optical/Infrared Ground-based Telescopes*. Edited by Iye, Masanori; Moorwood, Alan F. M. *Proceedings of the SPIE*, Volume 4841, pp. 1657-1669 (2003)., 1657–1669
- Faber, S. M. et al. 2005, *ApJ*, submitted, (astro-ph/0506044)
- Fukugita, M., Ichikawa, T., Gunn, J. E., Doi, M., Shimasaku, K., & Schneider, D. P. 1996, *AJ*, 111, 1748
- Gabasch, A., Bender, R., Seitz, S., Hopp, U., Saglia, R. P., Feulner, G., Snigula, J., Drory, N., Appenzeller, I., Heidt, J., Mehlert, D., Noll, S., Böhm, A., Jäger, K., Ziegler, B., & Fricke, K. J. 2004, *A&A*, 421, 41
- Gunn, J. E., Carr, M. A., Rockosi, C. M., Sekiguchi, M., et al. 1998, *AJ*, 116, 3040
- Hogg, D. W., Finkbeiner, D. P., Schlegel, D. J., & Gunn, J. E. 2001, *AJ*, 122, 2129
- Hogg, D. W. et al. 2004, *ApJ*, 601, L29
- Im, M., Simard, L., Faber, S. M., Koo, D. C., Gebhardt, K., Willmer, C. N. A., Phillips, A., Illingworth, G., Vogt, N. P., & Sarajedini, V. L. 2002, *ApJ*, 571, 136
- Kereš, D., Katz, N., Weinberg, D. H., & Davé, R. 2005, *MNRAS*, 363, 2
- Le Fèvre, O., Abraham, R., Lilly, S. J., Ellis, R. S., Brinchmann, J., Schade, D., Tresse, L., Colless, M., Crampton, D., Glazebrook, K., Hammer, F., & Broadhurst, T. 2000, *MNRAS*, 311, 565
- Lilly, S. J., Tresse, L., Hammer, F., Crampton, D., & Le Fèvre, O. 1995, *ApJ*, 455, 108
- Lin, L., Koo, D. C., Willmer, C. N. A., Patton, D. R., Conselice, C. J., Yan, R., Coil, A. L., Cooper, M. C., Davis, M., Faber, S. M., Gerke, B. F., Guhathakurta, P., & Newman, J. A. 2004, *ApJ*, 617, L9
- Lupton, R. H., Gunn, J. E., Ivezić, Z., Knapp, G. R., Kent, S., & Yasuda, N. 2001, in *ASP Conf. Ser. 238: Astronomical Data Analysis Software and Systems X*, Vol. 10, 269

- Nagamine, K., Cen, R., Hernquist, L., Ostriker, J. P., & Springel, V. 2005, *ApJ*, 618, 23
- Nagamine, K., Fukugita, M., Cen, R., & Ostriker, J. P. 2001, *MNRAS*, 327, L10
- Nagashima, M., Lacey, C. G., Okamoto, T., Baugh, C. M., Frenk, C. S., & Cole, S. 2005, *MNRAS*, 363, L31
- Patton, D. R., Pritchett, C. J., Carlberg, R. G., Marzke, R. O., Yee, H. K. C., Hall, P. B., Lin, H., Morris, S. L., Sawicki, M., Shepherd, C. W., & Wirth, G. D. 2002, *ApJ*, 565, 208
- Pier, J. R., Munn, J. A., Hindsley, R. B., Hennessy, G. S., Kent, S. M., Lupton, R. H., & Ivezić, Ž. 2003, *AJ*, 125, 1559
- Richards, G. et al. 2002, *AJ*, 123, 2945
- Schlegel, D. J., Finkbeiner, D. P., & Davis, M. 1998, *ApJ*, 500, 525
- Smith, J. A., Tucker, D. L., et al. 2002, *AJ*, 123, 2121
- Springel, V. & Hernquist, L. 2003, *MNRAS*, 339, 312
- Springel, V., White, S. D. M., Jenkins, A., Frenk, C. S., Yoshida, N., Gao, L., Navarro, J., Thacker, R., Croton, D., Helly, J., Peacock, J. A., Cole, S., Thomas, P., Couchman, H., Evrard, A., Colberg, J., & Pearce, F. 2005, *Nature*, 435, 629
- Stoughton, C. et al. 2002, *AJ*, 123, 485
- Strauss, M. A. et al. 2002, *AJ*, 124, 1810
- Terlevich, A. I., Caldwell, N., & Bower, R. G. 2001, *MNRAS*, 326, 1547
- Visvanathan, N. & Sandage, A. 1977, *ApJ*, 216, 214
- Willmer, C. N. A. et al. 2005, *ApJ*, submitted, (astro-ph/0506041)
- York, D. et al. 2000, *AJ*, 120, 1579

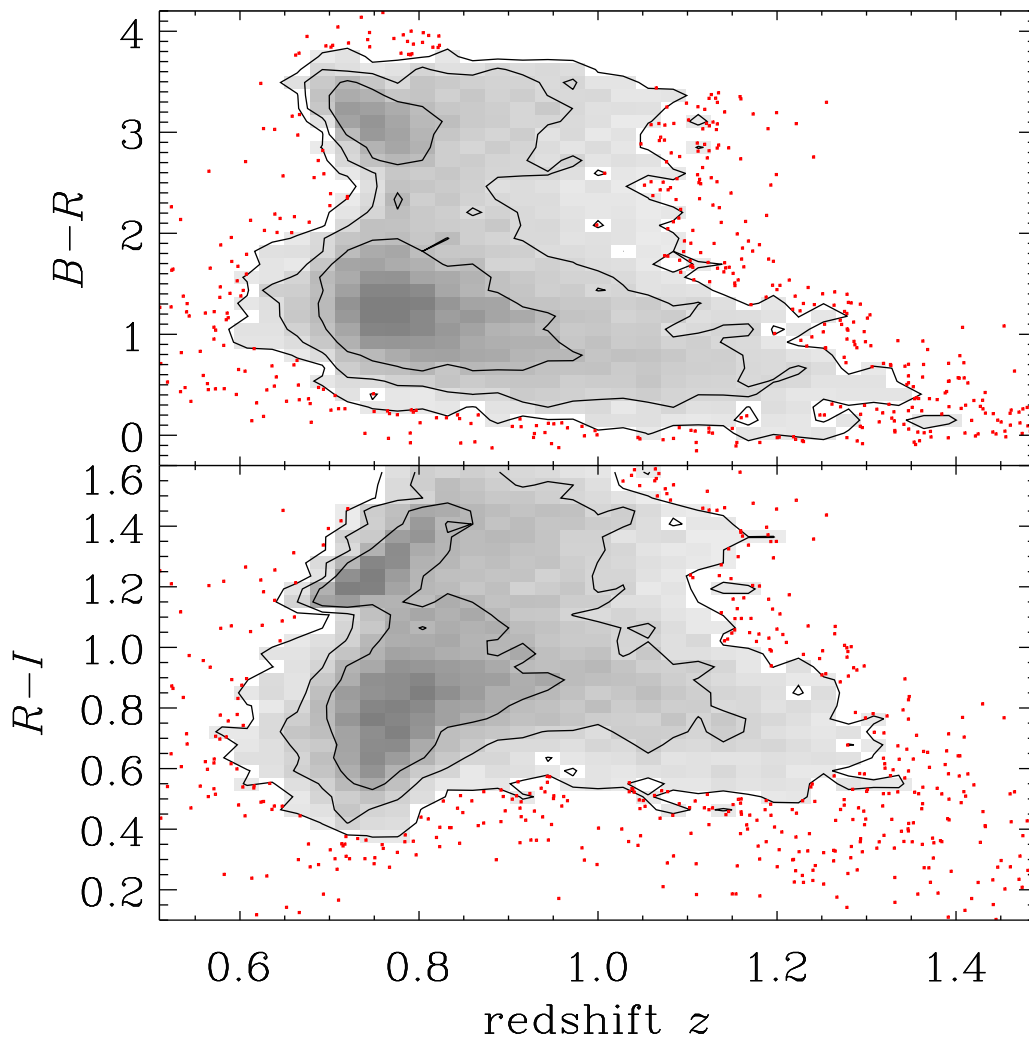


Fig. 1.— Predictions of DEEP2 colors from the local SDSS sample. The SDSS galaxies are redistributed in the range  $0.5 < z < 1.5$  uniformly in volume and  $B$ ,  $R$ , and  $I$  magnitudes are synthesized as described in the text. Greyscale indicates the density of galaxies in each bin of redshift and color. Contours enclose 52%, 84% and 97% of the galaxies, respectively. We show outlying galaxies as individual points.

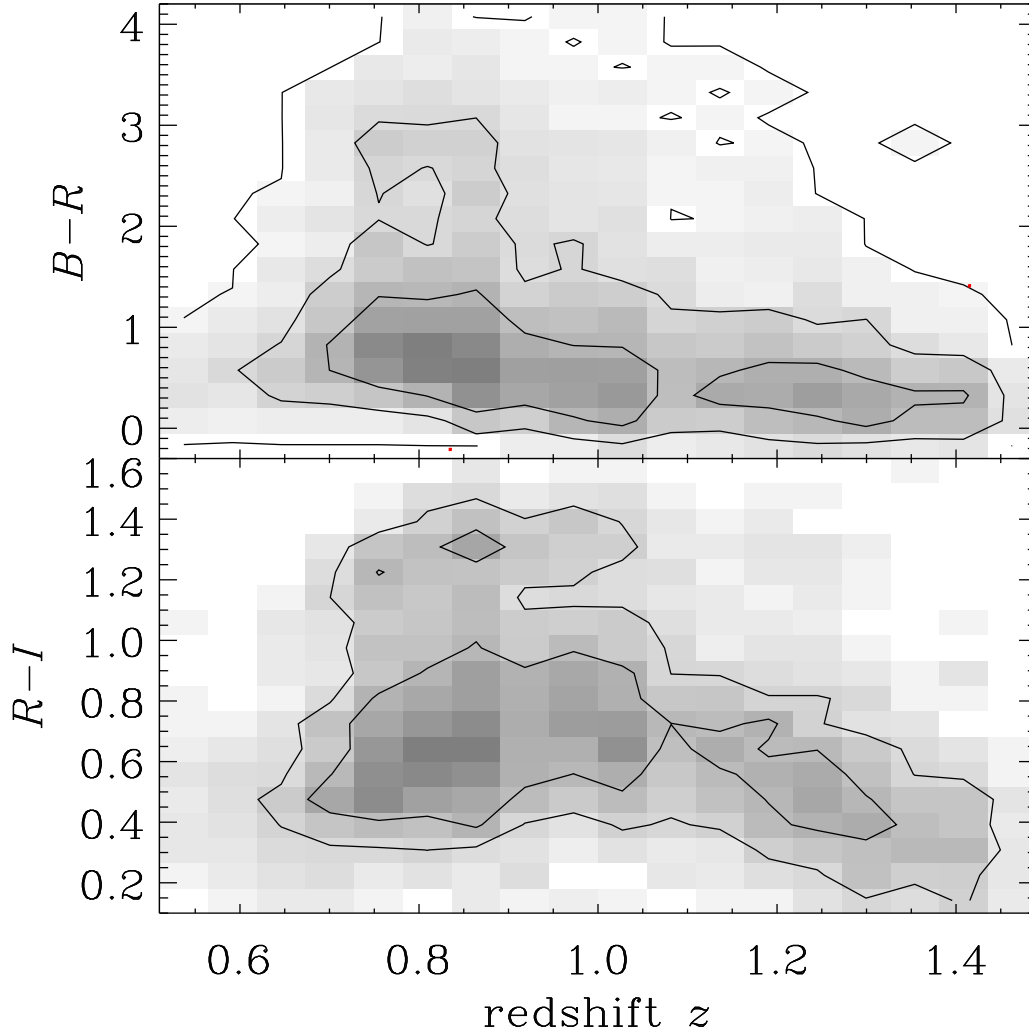


Fig. 2.— Same as Figure 1, for actual DEEP2 colors as a function of redshift. Obviously the galaxy population is far bluer than the prediction from low redshift — meaning galaxies at high redshift are far bluer than those today. As we show in Figures 3 and 4, the blue and red sequences are bluer at redshift  $z = 1$  than at  $z = 0.1$ , and in addition that the red sequence is much less well populated at higher redshift.

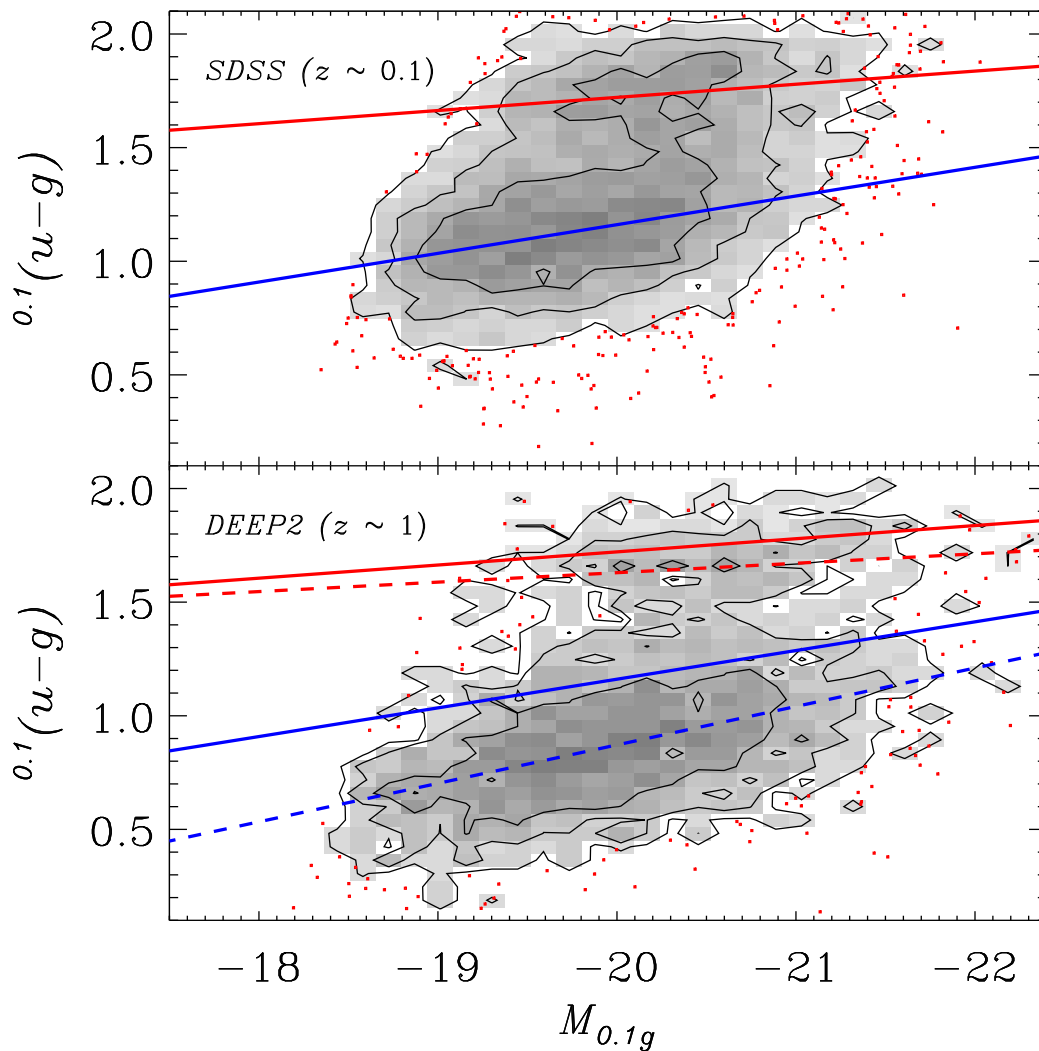


Fig. 3.— The SDSS-predicted (top panel) and observed (bottom panel) distribution of color and absolute magnitude. The prediction assumes no change in the galaxy population between redshifts  $z = 0.1$  and  $z = 1$ . The upper solid line in each panel is the locus of the red sequence in the SDSS prediction. The lower solid line is the locus of the blue sequence in the SDSS prediction. The dashed lines in the bottom panel are the corresponding loci in the DEEP2 data. The parameters of these fits are all in Table 1. The red sequence is far less well populated relative to the blue sequence at redshift  $z = 1$  than it is at redshift  $z = 0.1$ . In addition, the red and blue sequences are both bluer at high redshift than at low redshift.

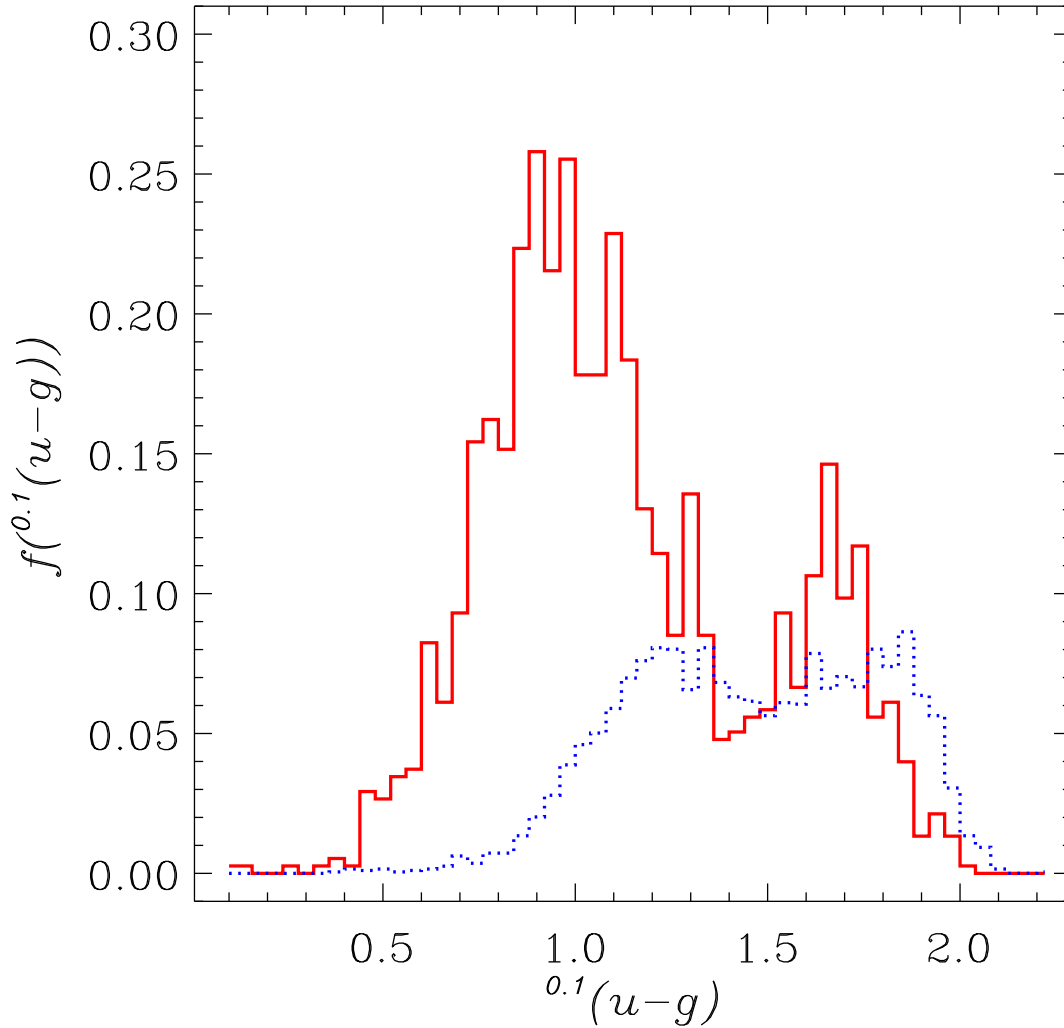


Fig. 4.— For luminous galaxies ( $M_{0.1g} - 5 \log_{10} h < -20$ ), the distribution of DEEP2 colors (solid histogram) compared to the SDSS prediction assuming no change in the population (dotted histogram). The curves are scaled such that the integrals are equal for  $^{0.1}(u-g) > 1.4$ . As Figure 3 shows, the blue population in DEEP2 is much bluer than its low redshift analog. In addition, the red sequence is slightly bluer (about 0.1 mag) and much less populated. In the DEEP2 sample, galaxies with  $^{0.1}(u-g) > 1.4$  comprise 24% of the sample, while in the SDSS prediction, galaxies with  $^{0.1}(u-g) > 1.5$  comprise 47% of the sample.

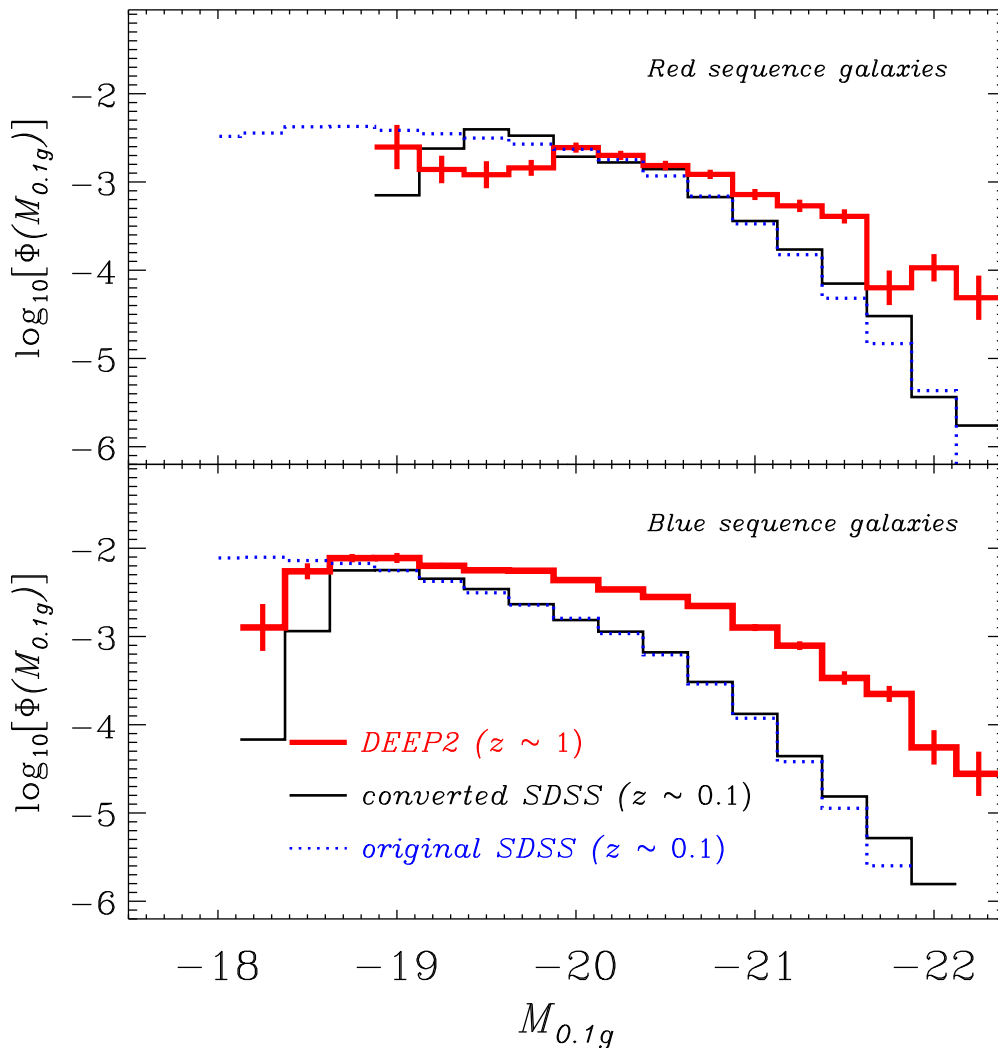


Fig. 5.— The luminosity function of red sequence galaxies (top panel) and blue sequence galaxies (bottom panel) in the  $^{0.1}g$  band. Each panel shows the luminosity function of galaxies in three ways: the redshift  $z \sim 0.1$  luminosity function of SDSS galaxies (dotted histogram); the redshift  $z \sim 0.1$  luminosity function of SDSS galaxies as it would be measured by a DEEP2-like survey (thin solid histogram); and the redshift  $z \sim 1$  luminosity function of DEEP2 galaxies. Where the two SDSS luminosity functions agree indicates where the DEEP2 luminosity function is unaffected by the explicit selection effects in DEEP2.

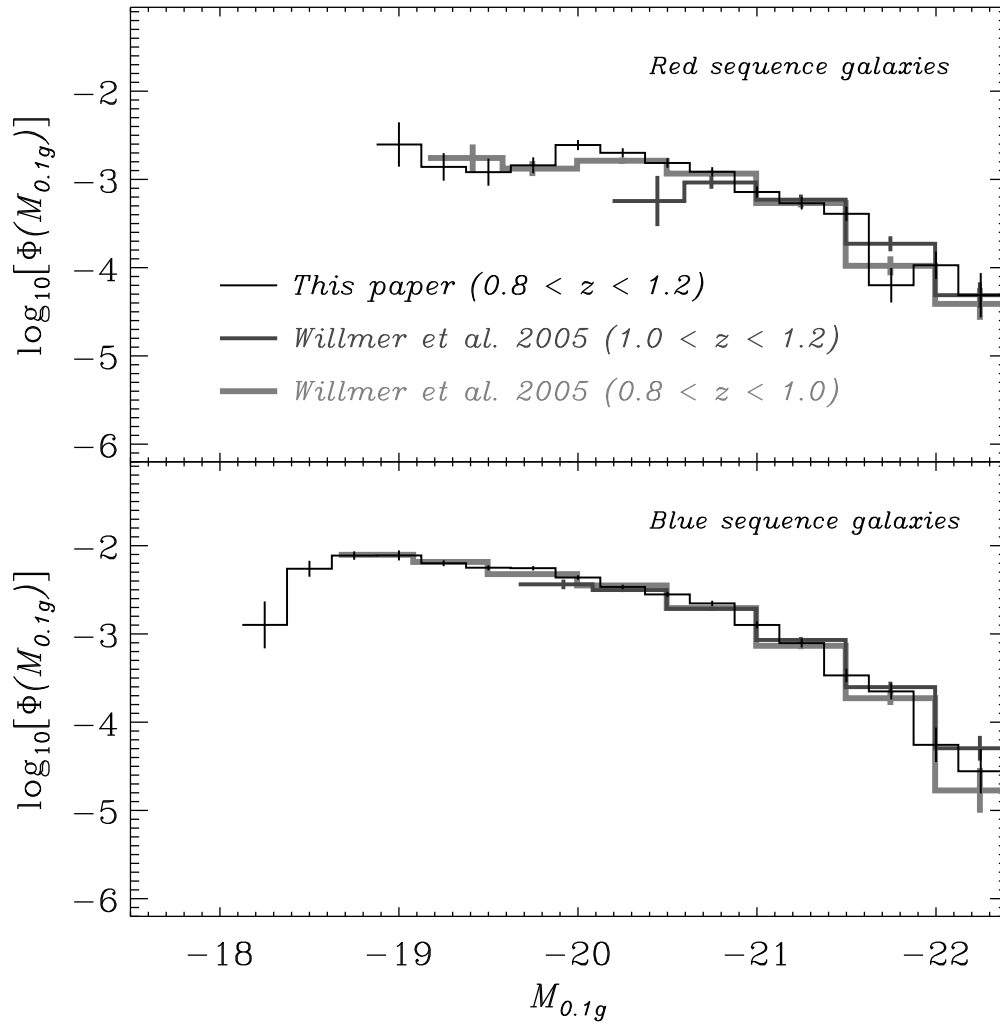


Fig. 6.— Similar to Figure 5, but only showing results for the DEEP2 survey. Our results are overlaid on those of Willmer et al. (2005), showing that they agree well.

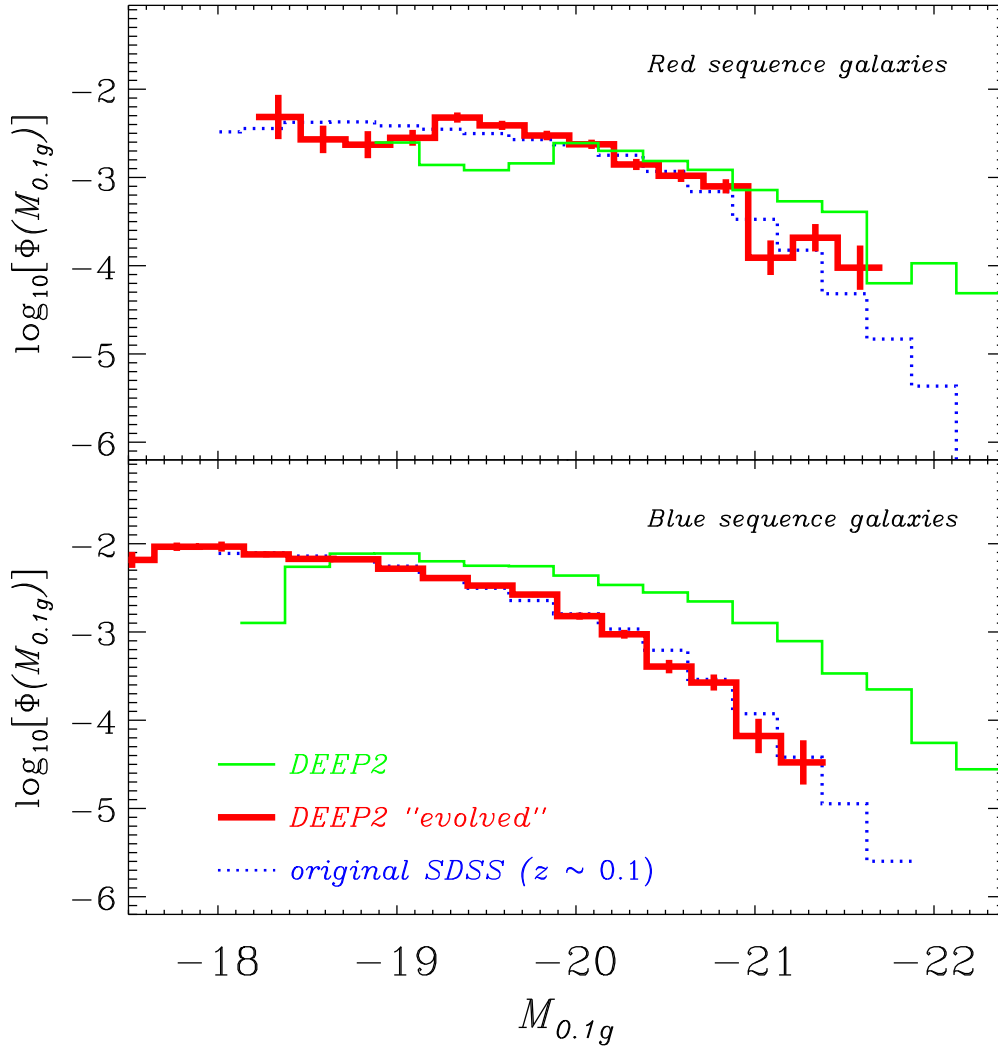


Fig. 7.— Similar to Figure 5. In addition to the original DEEP2 luminosity function (thin solid histogram), I show that luminosity function shifted according the parameters listed in Table 3 (thick solid histogram). The result matches the SDSS luminosity function reasonably well.

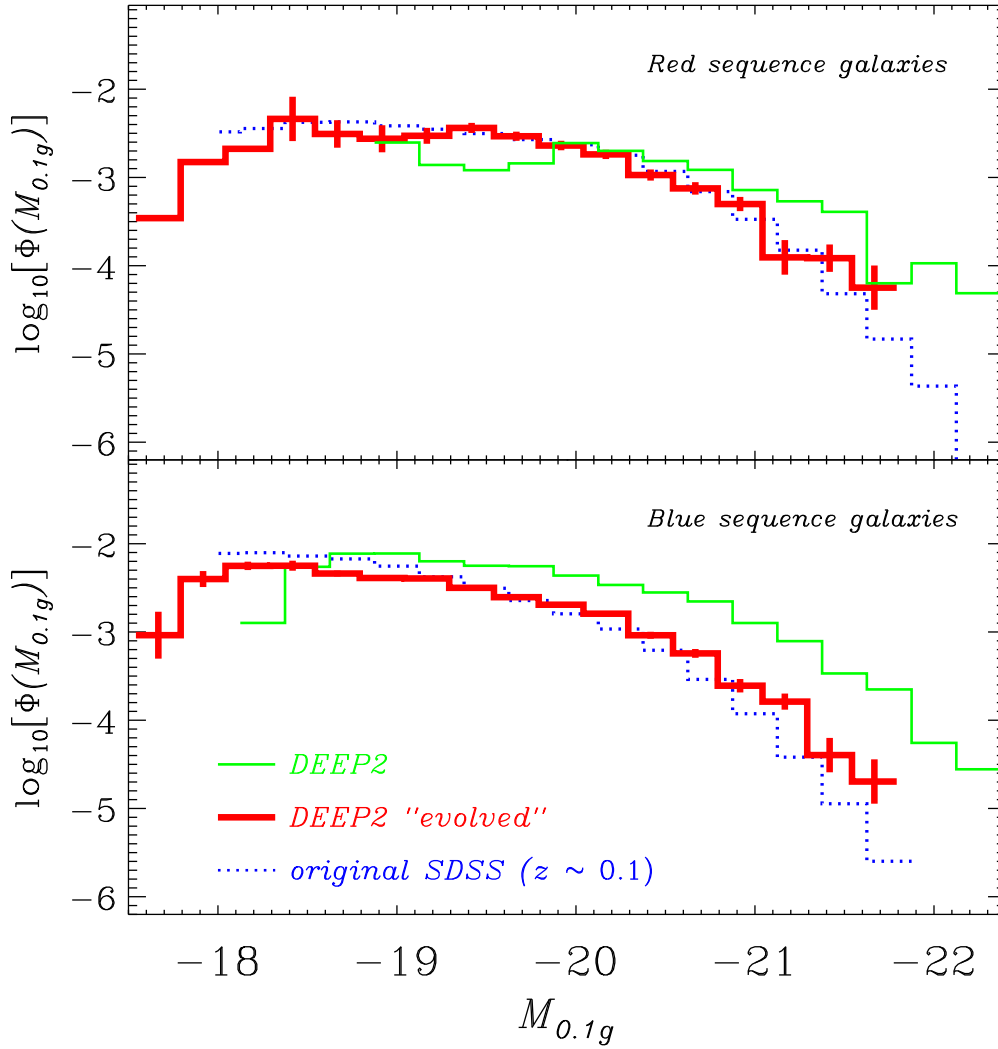


Fig. 8.— Similar to Figure 7. Now I show the result of allowing both luminosity functions to fade by about 0.6 mag, and transferring 25% of the blue galaxies from the blue to the red sequence (thick solid histogram). Again, this matches the SDSS luminosity function reasonably well.

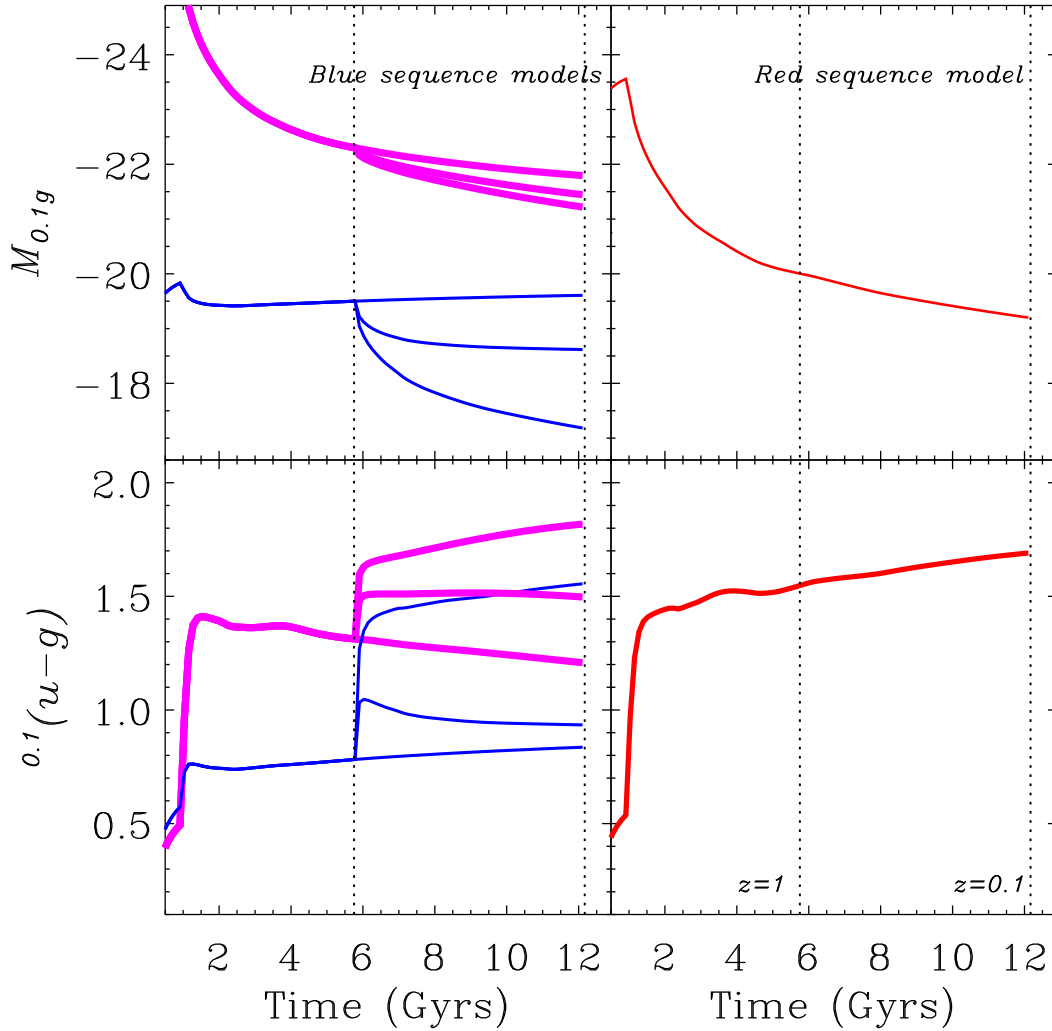


Fig. 9.— Colors and absolute magnitudes as a function of time, for models of the blue sequence (left panel) and red sequence (right panel) galaxies. The thick lines for the blue sequence galaxies correspond to a model with a large initial burst, the thin to a model with a small initial burst. The trifurcation at redshift  $z = 1$  indicates (from bottom to top) a continuation of star-formation at a constant rate, a decline in star-formation by a factor of three, and a complete cutoff in star-formation.

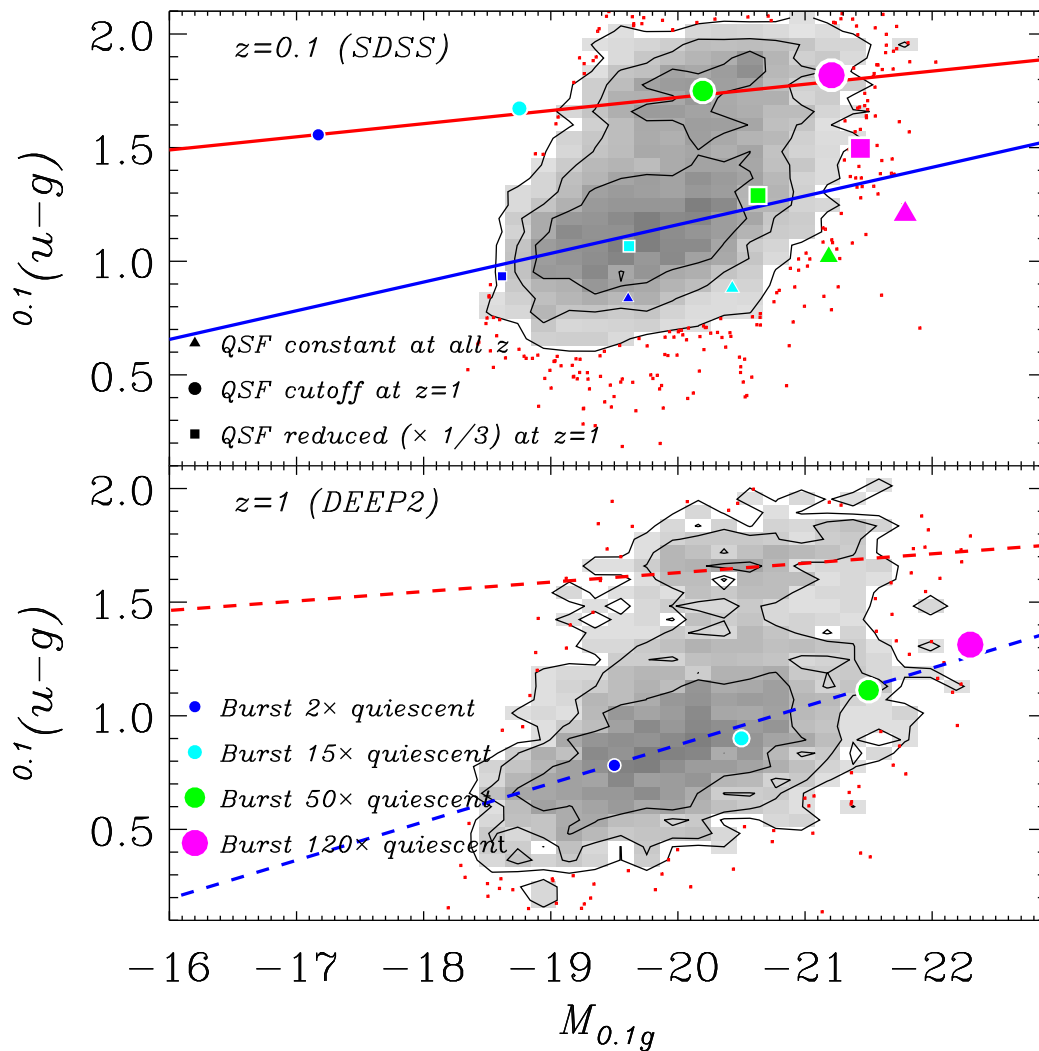


Fig. 10.— Same data as Figure 3, with some simple models overplotted (see Figure 9). Twelve models are presented in total, each consisting of a 1 Gyr burst starting at  $t = 0$  followed by quiescent star-formation (QSF) until at least redshift  $z = 1$  ( $t = 5.7$  Gyrs). There are four different burst strengths, shown with increasingly large symbols; for each burst strength the normalization is set to lie on the blue sequence at redshift  $z = 1$ . There are three different behaviors after redshift  $z = 1$ . For the circles, the quiescent star-formation cuts off at  $z = 1$ . For the squares, it is reduced by a factor of three. For the triangles, it continues until redshift  $z = 0$ . Each panel shows the color and magnitude of each model at the given redshift.

Table 1. Fits to color-magnitude relations

Survey	Color range	$a_0$	$a_1$
SDSS	$^{0.1}(u - g) > 1.5$	1.72	-0.06
—	$^{0.1}(u - g) < 1.5$	1.16	-0.13
DEEP2	$^{0.1}(u - g) > 1.4$	1.63	-0.04
—	$^{0.1}(u - g) < 1.4$	0.87	-0.17

Note. — Fits are of the form:  $^{0.1}(u - g) = a_0 + a_1(M_{0.1g} - 5 \log_{10} h + 20)$ .

Table 2. Luminosity functions

$M_{0.1g} - 5 \log_{10} h$	$\Phi$ (red, SDSS)	$\Phi$ (blue, SDSS)	$\Phi$ (red, DEEP2)	$\Phi$ (blue, DEEP2)
-23.50	—	—	—	—
-23.25	—	—	—	—
-23.00	—	—	—	—
-22.75	$(2.12 \pm 2.12) \times 10^{-7}$	—	—	—
-22.50	$(2.14 \pm 2.14) \times 10^{-7}$	—	—	—
-22.25	$(1.70 \pm 1.70) \times 10^{-7}$	—	$(488.11 \pm 282.00) \times 10^{-7}$	$(278.03 \pm 160.74) \times 10^{-7}$
-22.00	$(4.32 \pm 0.82) \times 10^{-6}$	—	$(106.62 \pm 38.12) \times 10^{-6}$	$(55.38 \pm 24.84) \times 10^{-6}$
-21.75	$(1.47 \pm 0.15) \times 10^{-5}$	$(0.25 \pm 0.06) \times 10^{-5}$	$(6.33 \pm 2.86) \times 10^{-5}$	$(22.35 \pm 4.69) \times 10^{-5}$
-21.50	$(4.81 \pm 0.26) \times 10^{-5}$	$(1.13 \pm 0.12) \times 10^{-5}$	$(40.74 \pm 7.56) \times 10^{-5}$	$(33.86 \pm 5.92) \times 10^{-5}$
-21.25	$(1.50 \pm 0.04) \times 10^{-4}$	$(0.38 \pm 0.02) \times 10^{-4}$	$(5.37 \pm 0.87) \times 10^{-4}$	$(7.87 \pm 0.90) \times 10^{-4}$
-21.00	$(3.36 \pm 0.07) \times 10^{-4}$	$(1.18 \pm 0.04) \times 10^{-4}$	$(7.21 \pm 1.05) \times 10^{-4}$	$(12.63 \pm 1.15) \times 10^{-4}$
-20.75	$(6.91 \pm 0.09) \times 10^{-4}$	$(2.90 \pm 0.06) \times 10^{-4}$	$(12.20 \pm 1.48) \times 10^{-4}$	$(22.17 \pm 1.54) \times 10^{-4}$
-20.50	$(1.17 \pm 0.01) \times 10^{-3}$	$(0.62 \pm 0.01) \times 10^{-3}$	$(1.53 \pm 0.19) \times 10^{-3}$	$(2.80 \pm 0.19) \times 10^{-3}$
-20.25	$(1.79 \pm 0.01) \times 10^{-3}$	$(1.08 \pm 0.01) \times 10^{-3}$	$(2.00 \pm 0.24) \times 10^{-3}$	$(3.41 \pm 0.20) \times 10^{-3}$
-20.00	$(2.35 \pm 0.02) \times 10^{-3}$	$(1.60 \pm 0.02) \times 10^{-3}$	$(2.45 \pm 0.32) \times 10^{-3}$	$(4.35 \pm 0.25) \times 10^{-3}$
-19.75	$(2.68 \pm 0.02) \times 10^{-3}$	$(2.27 \pm 0.02) \times 10^{-3}$	$(1.45 \pm 0.30) \times 10^{-3}$	$(5.56 \pm 0.33) \times 10^{-3}$
-19.50	$(3.15 \pm 0.03) \times 10^{-3}$	$(3.12 \pm 0.03) \times 10^{-3}$	$(1.21 \pm 0.43) \times 10^{-3}$	$(5.62 \pm 0.37) \times 10^{-3}$
-19.25	$(3.52 \pm 0.03) \times 10^{-3}$	$(4.21 \pm 0.04) \times 10^{-3}$	$(1.39 \pm 0.50) \times 10^{-3}$	$(6.32 \pm 0.48) \times 10^{-3}$
-19.00	$(3.84 \pm 0.04) \times 10^{-3}$	$(5.57 \pm 0.06) \times 10^{-3}$	$(2.49 \pm 1.44) \times 10^{-3}$	$(7.75 \pm 1.01) \times 10^{-3}$
-18.75	$(4.26 \pm 0.05) \times 10^{-3}$	$(6.72 \pm 0.09) \times 10^{-3}$	—	$(7.72 \pm 0.85) \times 10^{-3}$
-18.50	$(4.22 \pm 0.06) \times 10^{-3}$	$(7.25 \pm 0.12) \times 10^{-3}$	—	$(5.47 \pm 1.14) \times 10^{-3}$
-18.25	$(3.59 \pm 0.07) \times 10^{-3}$	$(7.91 \pm 0.18) \times 10^{-3}$	—	$(1.27 \pm 0.77) \times 10^{-3}$
-18.00	$(3.29 \pm 0.09) \times 10^{-3}$	$(7.76 \pm 0.29) \times 10^{-3}$	—	—

Note. —  $\Phi$  is number per  $h^{-3} \text{ Mpc}^3$  per unit magnitude. In SDSS, the division between red and blue is at  $^{0.1}(u - g) = 1.5$  and in DEEP2 it is at  $^{0.1}(u - g) = 1.4$ .

Table 3. Shifts in luminosity functions

Colors	$\Delta M_{0.1g} = M_{0.1g,SDSS} - M_{0.1g,DEEP2}$	$f_{\text{off}} = \rho_{SDSS}/\rho_{DEEP2}$	$r$
Blue	$0.98 \pm 0.09$	$1.20 \pm 0.14$	0.45
Blue (shift fixed)	0.90	$1.13 \pm 0.13$	—
Red	$0.66 \pm 0.04$	$1.95 \pm 0.20$	0.28
Red (shift fixed)	0.80	$2.14 \pm 0.22$	—

Note. — The “shift fixed” cases have  $\Delta M_{0.1g}$  fixed to a reasonable value based on stellar population synthesis models.  $r$  is the correlation coefficient between the errors in the shift  $\Delta M_{0.1g}$  and the offset  $f_{\text{off}}$ .